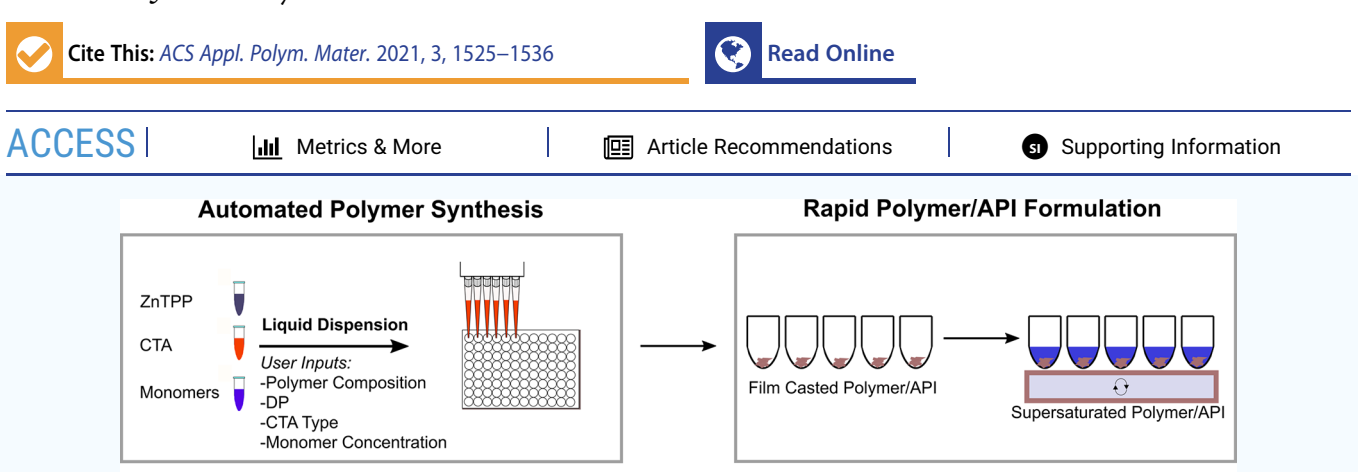


pubs.acs.org/acsapm Article

Automated PET-RAFT Polymerization toward Pharmaceutical Amorphous Solid Dispersion Development

Rahul Upadhya, Ashish Punia,* Mythili J. Kanagala, Lina Liu, Matthew Lamm, Timothy A. Rhodes, and Adam J. Gormley*



ABSTRACT: In pharmaceutical oral drug delivery development, about 90% of drugs in the pipeline have poor aqueous solubility leading to severe challenges with oral bioavailability and translation to effective and safe drug products. Amorphous solid dispersions (ASDs) have been utilized to enhance the oral bioavailability of poorly soluble active pharmaceutical ingredients (APIs). However, a limited selection of regulatory-approved polymer excipients exists for the development and further understanding of tailor-made ASDs. Thus, a significant need exists to better understand how polymers can be designed to interact with specific API moieties. Here, we demonstrate how an automated combinatorial library approach can be applied to the synthesis and screening of polymer excipients for the model drug probucol. We synthesized a library of 25 random heteropolymers containing one hydrophilic monomer (2-hydroxypropyl acrylate (HPA)) and four hydrophobic monomers at varied incorporation. The performance of ASDs made by a rapid film casting method was evaluated by dissolution using ultra-performance liquid chromatography (UPLC) sampling at various time points. This combinatorial library and rapid screening strategy enabled us to identify a relationship between polymer hydrophobicity, monomer hydrophobic side group geometry, and API dissolution performance. Remarkably, the most effective synthesized polymers displayed slower drug release kinetics compared to industry standard polymer excipients, showing the ability to modulate the drug release profile. Future coupling of high throughput polymer synthesis, high throughput screening (HTS), and quantitative modeling would enable specification of designer polymer excipients for specific API functionalities.

KEYWORDS: oral drug delivery, combinatorial polymer synthesis, amorphous solid dispersions, drug precipitation inhibition, polymer excipients

1. INTRODUCTION

Among the numerous routes of pharmaceutical drug administration, oral drug delivery is the most prevalent because of its simplicity and high patient compliance. 1,2 Oral drugs are classified by the Biopharmaceutics Classification System (BCS) which categorizes drugs into four groups based on water solubility and permeability across the intestinal mucosal barrier. 1,3 Bioactive pharmaceuticals are often identified via high throughput screening (HTS) whereby automated and quantitative design techniques are employed. 4-7 HTS will often hone in on hydrophobic drug candidates because hydrophobic interactions play a major role in drug-receptor binding. 1,8,9 In fact, 40% of oral drugs on the market are poorly soluble (BCS Class II or IV) while about 90% of those in development have

low solubility.^{1,3,10,11} The poor aqueous solubility of the majority of drug candidates leads to severe challenges with oral bioavailability and translation to an effective oral dosage form within safe dosage limits.

To address these challenges, amorphous solid dispersion (ASD) formulation via spray drying or hot melt extrusion is widely used. ASDs increase aqueous solubility by molecularly

Received: December 14, 2020 Accepted: February 4, 2021 Published: February 15, 2021





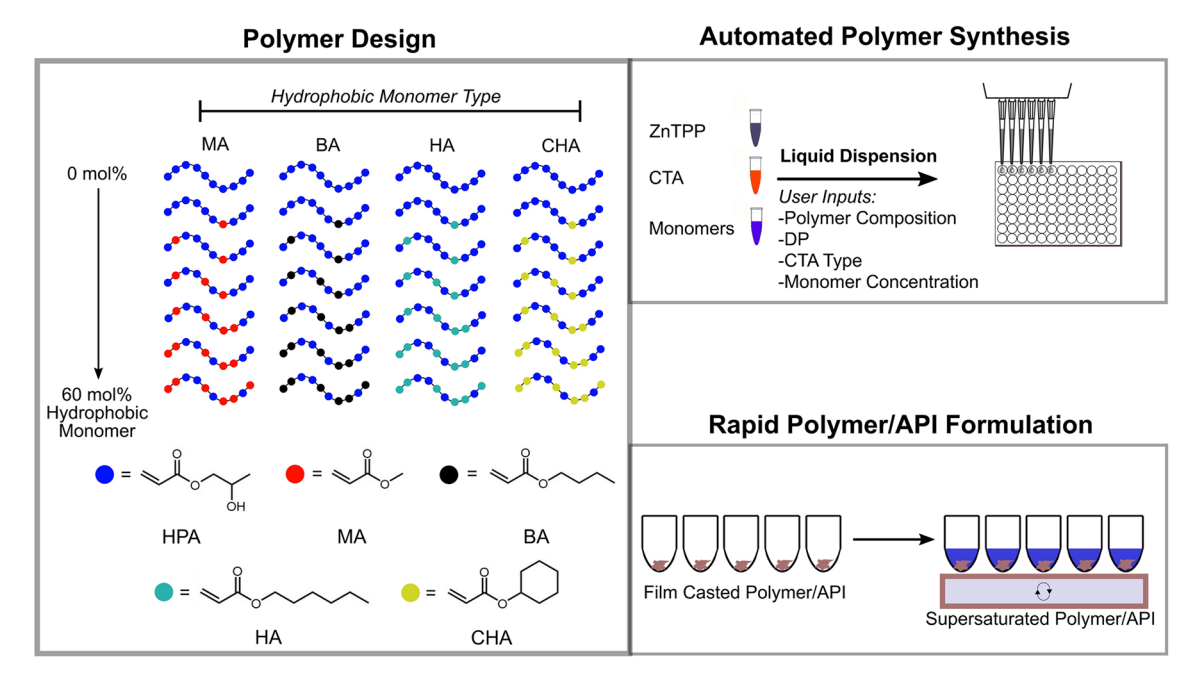


Figure 1. Experimental design schematic. Polymers were designed to participate in polar and nonpolar interactions with the model drug probucol. In these random heteropolymers, a hydrophilic monomer (HPA) was copolymerized with 0–60 mol % of hydrophobic monomers (MA, BA, HA, and CHA). Automated polymer synthesis was conducted with liquid handling robotics to dispense correct volume of monomer, CTA, and initiator into 96-well plates. Formulation of polymer/API was assessed by a film casting screening experiment. Further characterization of polymer/API miscibility and crystallization was completed by using mDSC, XRD, and polarized light microscopy.

dispersing active pharmaceutical ingredients (APIs) in an amorphous polymer with a high glass transition temperature $(T_{\rm g})$. $T_{\rm g}$. Despite the diversity of published work studying polymer structures, ^{15–20} lipid-based delivery systems, ^{2,21,22} microencapsulations, ²³ hydrogels, ²⁴ and natural polymers, ^{25–28} the vast majority of ASD formulations utilize cellulose-derived polymers such as hydroxypropyl methylcellulose (HPMC) and hydroxypropyl methylcellulose acetate succinate (HPMCAS). ^{29–33} By limiting the diversity of available polymer excipient designs, few commercial options are available for particularly problematic APIs. Therefore, a need exists in the oral drug delivery community to better understand how excipients can be tailor-made for specific APIs. Distinct structural attributes such as molecular weight, dispersity (D), and comonomer distribution can impact both the physical stability and solution performance of ASDs. A systematic approach toward understanding how polymer attributes impact ASD performance is needed as well as a robust approach toward designing tailor-made ASDs.

Synthetic polymers are uniquely equipped to meet this need as structural parameters such as degree of polymerization (DP), monomer composition, architecture (e.g., linear vs star-shaped), and functionalization can be controlled.^{34–39} Traditional controlled living radical polymerization (CLRP) techniques such as reversible addition—fragmentation chain-transfer (RAFT) polymerization and atom transfer radical polymerization (ATRP) suffer from the requirement to provide inert reaction conditions by degassing.^{40,41} Practically, this has prevented the synthesis of large and precisely designed combinatorial polymer libraries. Consequently, these laborintensive techniques have delayed full exploration of polymer structural traits and ultimately excipient design parameters for specific API moieties.^{15–19,42–44}

Recently, oxygen-tolerant techniques have been developed by our group and others to carry out efficient polymerizations in 96well plates. This includes enzyme-assisted initiators for continuous activator regeneration (ICAR) ATRP, ⁴⁵ enzyme-assisted RAFT (Enz-RAFT), ^{46,47} and photoinduced electron transfer-RAFT (PET-RAFT). ⁴⁸ Numerous publications have utilized PET-RAFT in particular to synthesize polymers in DMSO at low volume. ^{49–51} We have previously used PET-RAFT to undertake structure–function testing of polymer designs from combinatorial libraries. ^{38,52} This ability to conduct polymerizations at the benchtop has enabled robotic automation of Enz-RAFT and PET-RAFT with a user-friendly interface, time and labor savings, and experimental reproducibility. ⁵³

Reineke, Hillmyer, and others have previously explored various polymer chemistries for designing ASDs of model drugs such as probucol and phenytoin, also employing an automated synthesis and rapid screening process. 15,17-20,42 Our goal was to further improve upon this throughput capability by exhibiting the utility of an automated air-tolerant polymer synthesis approach that can be conducted directly in 96-well plates. Here, we demonstrate that an automated combinatorial polymer synthesis approach can be combined with high throughput ASD excipient screening to reveal the effect of polymer design parameters on API dissolution performance (Figure 1). Specifically, we investigated the effect of copolymer amphiphilicity (side group length and mole ratio) and geometric shape (linear vs cyclic) of hydrophobic side groups on the dissolution enhancement of model API probucol (BCS Class II). We synthesized random heteropolymers containing a hydrophilic monomer 2-hydroxypropyl acrylate (HPA) and hydrophobic monomers at varied incorporation (0-60 mol %) including methyl acrylate (MA), butyl acrylate (BA), hexyl acrylate (HA), and cyclohexyl acrylate (CHA). HPA was selected to potentially engage in hydrogen bonding with the API while MA, BA, HA, and CHA were selected to tune hydrophobicity. The effect of hydrophobic monomer side chain geometry was investigated by evaluating the performance of polymers with linear hexyl side

chains to polymers with a cyclohexyl side chain (CHA) at a range of mole ratios. A combinatorial library of 25 polymers was synthesized in 96-well plates via automated PET-RAFT using a Hamilton Microlab STARlet liquid handling robot. Initial characterization was completed by gel permeation chromatography (GPC) and modulated differential scanning calorimetry (mDSC) to quantify molecular weight, D, and glass-transition temperature (T_o). ASD screening was utilized to rapidly assess this polymer library toward enhancement of dissolution performance of the hydrophobic model API probucol. For comparison, industry standard polymers HPMCAS, HPMC, and vinylpyrrolidone-vinyl acetate copolymer (PVP/VA) were also investigated for probucol supersaturation. The ASD screen included preparation of solvent-cast polymer/drug mixtures, reconstitution in biorelevant media, and quantification of dissolved probucol concentration at various time points by ultra-performance liquid chromatography (UPLC). Physical characterization of solvent-cast polymer/drug was performed by mDSC, transmission X-ray diffraction (XRD), and polarized light microscopy to verify the amorphous or crystalline nature of the API and miscibility of the polymers with API. By taking advantage of automated open-air PET-RAFT via the adaptation of liquid handling robotics, we can synthesize a large combinatorial library of polymer excipients for oral drug delivery formulations directly in 96-well plates and therefore identify insightful polymer structure—activity relationships.

2. EXPERIMENTAL SECTION

- **2.1. Materials.** Monomers HPA, MA, BA, HA, and CHA were purchased from Polysciences, VWR, Sigma-Aldrich, and Fisher Scientific, respectively. The chain transfer agent (CTA) 4-cyano-4-[(dodecylsulfanylthiocarbonyl)sulfanyl]pentanoic acid was purchased from Sigma-Aldrich while the initiator ZnTPP was from Tokyo Chemical Industry Co., Ltd. Prior to handling, all monomers were deinhibited by pipetting over a column of inhibitor removal beads (Sigma-Aldrich). Monomer aliquots were made at 2 M, CTA aliquots at 50 mM, and zinc tetraphenylporphyrin (ZnTPP) aliquots at 2 mM in DMSO. The industry standard polymers used as controls were HPMCAS, HPMC, and the vinylpyrrolidone—vinyl acetate copolymer (PVP/VA). Three water-soluble grades of HPMCAS (Shin-Etsu AQOAT) were utilized: LF, MF, and HF. HPMC (Shin-Etsu PHARMACOAT) 603 grade was also used. PVP/VA was sourced from BASF. Probucol was purchased from Combi-Blocks (98% purity).
- **2.2. Automated PÉT-RAFT.** One milliliter aliquots of all monomers, CTA, and ZnTPP were loaded into the Hamilton Microlab STARlet automated liquid handling robot along with a 96-well polypropylene plate. ⁵³ Homopolymers and random heteropolymers were synthesized at a fixed DP of 200 (monomer:CTA ratio of 200:1) while the CTA:ZnTPP ratio was fixed at 100:1. The polymer composition was such that there was a hydrophilic monomer (HPA) along with varied incorporation of hydrophobic monomer (0–60 mol %). For the purpose of synthesizing a large quantity of polymer, reaction volumes were prepared in triplicate. Once solutions were transferred into their respective wells of the 96-well plate, the plate was sealed with film (VWR), and the polymerization was initiated by irradiation with a 560 nm LED light for 6 h.
- **2.3. Polymer Purification and Preparation.** For purification of polymers, Zeba spin desalting plates (Thermo Fisher Scientific) were manually loaded with Sephadex G-25 superfine resin which has a molecular weight cutoff (MWCO) of 5 kDa. The resin was stored in DMSO for 6 h to swell prior to use. The protocol which includes wash steps, sample loading volumes, and centrifugation rate was consistent with a previous study from our group. ⁵⁴ Purified polymers were diluted 3× in DMSO and then an additional 3× in ultrapure water. Diluted polymers were then dialyzed by using Spectra/Por regenerated cellulose prewetted dialysis tubing (Repligen) with a MWCO of 1

kDa. Dialysis was completed after 12 h, at which point polymers were lyophilized in 15 mL centrifuge tubes.

- **2.4. Gel Permeation Chromatography (GPC).** Once synthesized, polymers were characterized by GPC to obtain molar mass and dispersity (\mathcal{D}). Polymers were diluted to 2 mg/mL in DMF and filtered by using 0.45 μ m PTFE filters. We used an Agilent 1200 Series system equipped with UV and differential refractive index (RI) detectors with a DMF/LiBr mobile phase. Two organic size-exclusion Phenomenex Phenogel columns (10^4 and 10^3 Å) were used for molecular weight analysis by correlating to the measured RI response of poly(ethylene oxide) (PEO) standards in DMF without correction.
- 2.5. Film Casting Screen. A stock solution of probucol was prepared at 6.67 mg/mL in acetone and added to solid preweighed out polymers such that polymer concentration was 26.67 mg/mL (20% drug loading). Individual polymer/drug solutions were agitated by vortexing, and then 125 μ L was dropped into round-bottom glass vials. After leaving overnight and allowing acetone to fully evaporate, we observed films of polymer/drug. One milliliter of 0.5% fasted state simulated intestinal fluid (FaSSIF) in PBS (pH 6.5) was added to each vial such that the target drug concentration was 834 μ g/mL. Vials were constantly agitated at a rate of 500 rpm at 26 °C. At various sampling time points (15, 30, 90, 210, and 330 min), $100 \mu L$ was obtained from each vial by using multichannel pipettes and added to filter plates (Waters Corporation). To remove any precipitates, filter plates were centrifuged at 4100 rpm for 8 min. Filtrate was then diluted 3× in buffer (40:40:20 MeOH:MeCN:H2O with 0.1% w/v phenol internal standard) and sealed in deep-well 96-well plates.
- **2.6. Ultra-Performance Liquid Chromatography (UPLC).** UPLC was completed on a Waters ACQUITY H-Class system which enabled direct loading of covered deep well 96-well plates from the film casting screen. We employed the Waters ACQUITY UPLC BEH C18 column (2.1 \times 30 mm, 1.7 μ m pore size) which was maintained at 40 °C. With a flow rate of 0.8 mL/min and injection volume of 1 μ L, two mobile phases were used (A was H₂O/0.1% TFA, and B was acetonitrile/0.1% TFA). In our method, initial conditions were 90% solvent A, shifting to 10% solvent A at 1 min, held at 10% solvent A until 1.8 min, shifted to 90% solvent A at 2.1 min, and held at 90% solvent A until 2.5 min. The Waters ACQUITY UV detector collected data at 254 nm.
- 2.7. Modulated Differential Scanning Calorimetry (mDSC). Three groups of samples were run by mDSC on a TA Discovery DSC with slightly different methods: polymers, solvent-cast polymer/drug, and probucol. Each individual polymer was weighed out to about 5 mg and loaded into Tzero hermetically sealed pans with Tzero lids (TA Instruments). The mDSC system was equilibrated to -50 °C and maintained at this temperature for 5 min. A temperature ramp of 2 °C/ min (0.5 °C amplitude and 60 s period) was started until the system reached 200 °C, at which point a temperature ramp of -20 °C/min was applied until the system reached -50 °C. The second heat cycle was analyzed to quantify T_a of polymers. For polymer/drug films, 100 μ L of polymer/drug mixture in acetone was pipetted into the same DSC pans (30 μ L maximum at a time) and given time overnight to completely evaporate. After the instrument equilibrated at -50 °C, a temperature ramp of 2 °C/min (0.5 °C amplitude and 60 s period) was applied until the system was at 155 °C. A temperature ramp of -20 °C/min was applied until the system was equilibrated back to $-50\,^{\circ}$ C. An additional temperature ramp up to 155 °C was then administered. For probucol, about 5 mg of API was weighed out into DSC pans. From −50 °C, the temperature was ramped up at 2 °C/min to 150 °C, at which point a sudden temperature decrease to $-50\,^{\circ}\text{C}$ was applied and held for 5 min. The ramp up of temperature to 150 °C was increased for a second heat
- **2.8. Transmission X-ray Diffraction (XRD).** A total of $100 \,\mu\text{L}$ (20 μL pipetted at a time) of polymer/drug mixture in acetone was dropped into each well of a 96-well Kapton tape plate. These wells were left overnight before analysis to ensure full evaporation of acetone. X-ray analysis was conducted on samples in 96-well plates with a Bruker D8 Discover using Cu K α radiation (1.54 Å; 50 kV × 1000 mA) with a Vantec 500 area detector via transmission mode for 150 s. The 2D patterns were integrated from 4.0° to 38.0° 2θ .

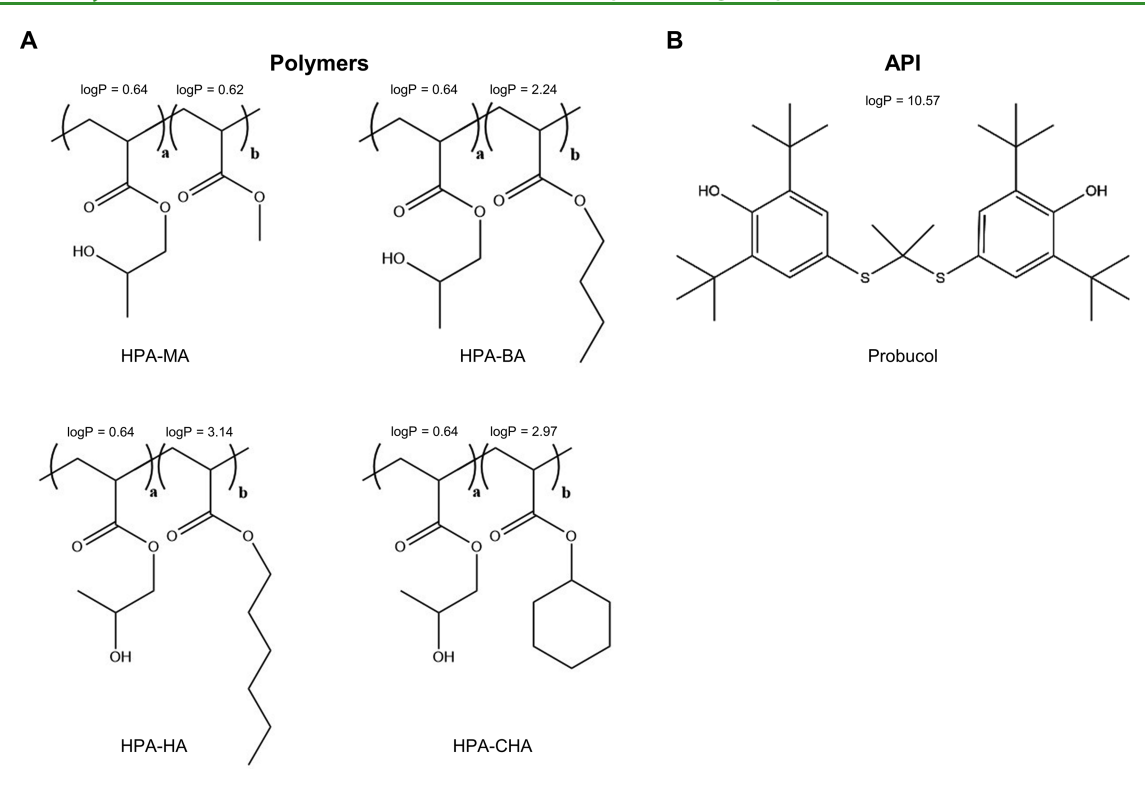


Figure 2. Schematic of polymers and model API. (A) Structures of all random heteropolymers that contained hydrophilic monomer HPA (group a) with hydrophobic monomers MA, BA, HA, and CHA (group b) incorporated at 0-60 mol %. (B) Structure of model API probucol. Note that the log P values of monomers and probucol are included above the structures.

Table 1. Characterization Data for All Synthesized Polymers

polymer	$\log P$	$T_g (^{\circ}C)^a$	MW _{theor} (Da)	$MW_{GPC} (Da)^{b}$	$\mathcal{D}_{\mathrm{GPC}}^{}^{}}}$	MW_{NMR}^{c} (Da)	hydrophobic mol incorporation $(\%)^c$
HPA	0.64	23	26028	19601	1.16	22854	0
HPA-MA 10%	0.64	23	25147	18048	1.18	15924	12.7
HPA-MA 20%	0.64	22	24266	16451	1.14	17886	25.9
HPA-MA 30%	0.63	22	23385	16110	1.14	15276	39.3
HPA-MA 40%	0.63	21	22504	14356	1.16	13892	45.3
HPA-MA 50%	0.63	20	21623	12969	1.14	17252	54.8
HPA-MA 60%	0.63	19	20742	12302	1.08	13960	63.7
HPA-BA 10%	0.80	18	25989	18730	1.15	15551	10.6
HPA-BA 20%	0.96	12	25949	18090	1.19	15517	25.0
HPA-BA 30%	1.12	6	25910	16864	1.15	12977	30.2
HPA-BA 40%	1.28	0	25870	16630	1.17	15030	40.9
HPA-BA 50%	1.44	-8	25831	16759	1.20	14954	50.2
HPA-BA 60%	1.60	-17	25792	14633	1.10	14145	59.5
HPA-HA 10%	0.89	15	26549	18993	1.17	18731	16.1
HPA-HA 20%	1.14	7	27070	18311	1.18	16558	27.4
HPA-HA 30%	1.39	-1	27592	17607	1.16	19800	35.9
HPA-HA 40%	1.64	-9	28113	16878	1.14	17426	47.4
HPA-HA 50%	1.89	-19	28634	13740	1.16	13673	58.5
HPA-HA 60%	2.13	27	29155	_ <i>d</i>	_ ^d	_ ^d	_d
HPA-CHA 10%	0.87	24	26790	17579	1.26	15754	15.6
HPA-CHA 20%	1.11	25	27552	18999	1.18	19107	16.4
HPA-CHA 30%	1.34	27	28313	17374	1.17	22949	38.9
HPA-CHA 40%	1.57	27	29075	16061	1.16	22243	49.4
HPA-CHA 50%	1.81	29	29837	15405	1.16	18851	58.3
HPA-CHA 60%	2.04	30	30599	12541	1.19	25418	67.9

^aDetermined by the second heat cycle by mDSC. ^bDetermined by GPC with DMF/LiBr as the mobile phase. ^cQuantified by ¹H NMR end-group analysis. ^dDid not polymerize.

2.9. Polarized Light Microscopy. A total of 100 μ L (20 μ L at a time) of polymer/drug mixture in acetone was dropped onto individual

glass microscope slides which were left on the benchtop until the acetone completely evaporated. A ZEISS microscope equipped with an

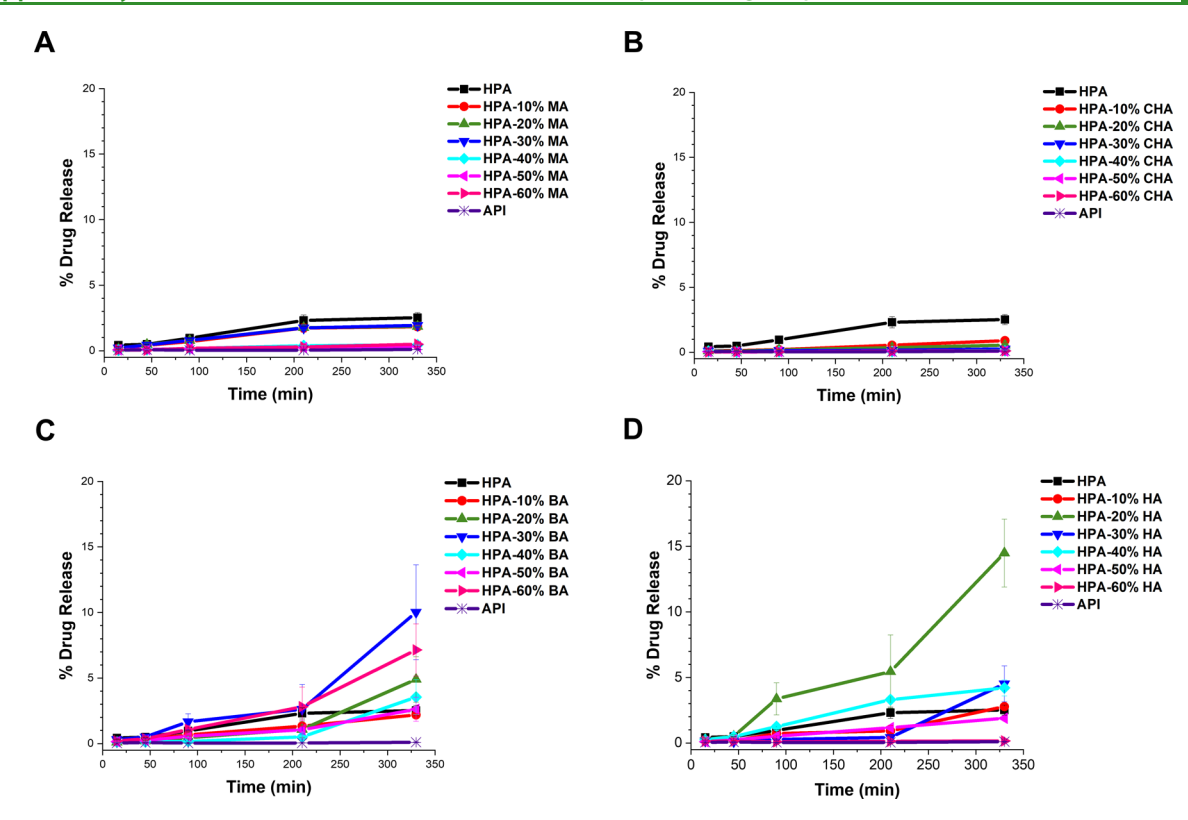


Figure 3. Dissolution plots demonstrating the effect of hydrophobic monomer incorporation. Plots contain hydrophilic monomer HPA along with 10–60 mol % of hydrophobic monomers (A) MA, (B) CHA, (C) BA, and (D) HA. As shown, the API was also film casted in the same manner but without polymer excipient. Drug release was quantified by UPLC and obtained by comparison to API standard injections (final concentration of 834 μ g/mL). Film casting was completed in triplicate, and the error bars represent the standard error.

AxioVision 4 stage was utilized to collect polarized light microscopy images. For the images collected, a 5× magnification was used and a 200 $\mu \rm m$ scale bar was selected. No further corrections or image processing was completed.

3. RESULTS AND DISCUSSION

First, we rationally designed a polymer library of random heteropolymers to serve as excipients for the model drug probucol (Figure 2). The octanol—water partition coefficient (log P) is a measure of hydrophobicity such that the log P of 10.57 for probucol indicates that it has poor aqueous solubility. Furthermore, probucol has a low measured solubility of 4.0 μ g/mL in FaSSIF (pH 6.5) and is regarded as a slow crystallizer with a melting temperature ($T_{\rm m}$) of 125 °C. There is evidence to suggest that hydrogen-bonding interactions involving hydroxyl groups contribute to probucol crystallization. Therefore, we selected HPA as the hydrophilic monomer since it contains a hydroxyl side group. Because probucol is poorly soluble, we tuned polymer hydrophobicity by selecting the comonomers MA, BA, HA, and CHA.

Random heteropolymers with a DP of ~200 were first synthesized by automated PET-RAFT whereby all reagent additions were completed in a 96-well plate by using the Hamilton Microlab STARlet liquid handling robot. ⁵³ Once synthesized, these polymers were characterized by GPC and mDSC to obtain the molecular weight, D, and $T_{\rm g}$ (Table 1). The GPC chromatograms and corresponding signal-to-noise information are available in Figure S2 and Table S1 of the Supporting Information. Polymers are named with the hydrophilic (HPA) and hydrophobic (MA, BA, HA, or CHA) monomers along with a percentage that represents feed mol % of

hydrophobic monomer. An example polymer structure including CTA is shown in Figure S1. The molecular weight reported is the weight-average molecular weight (M_w) based on calibration with PEO standards, while $T_{\rm g}$ values that are reported were obtained by analyzing the second heat cycle of DSC. The second heat cycle T_g was measured to remove effects from residual or absorbed moisture content during storage to enable assessment of polymers' inherent T_g without significant effect from thermal history or variable moisture content. We achieved controlled polymerization as D < 1.26 in all polymers. We further list calculated log *P* of the respective monomer compositions. This was done in the same way as a previous publication in which we calculated the weighted average of two monomer log P values based on mol % of each monomer. 52 Lastly, the number-average molecular weight and hydrophobic monomer incorporation are included as determined by ¹H NMR end-group analysis (see section S5 and Figures S12-S15 in the Supporting Information).

We then assessed the ability of polymers to achieve supersaturation of the hydrophobic API probucol via a rapid film casting ASD screening experiment. The 25 polymers along with standard polymer excipients (PVP/VA and HPMCAS) were mixed with drug in acetone at 20 wt % drug loading. Once the solvent was fully evaporated, each film was dissolved in FaSSIF and sampled at various time points (15, 45, 90, 210, and 330 min) to determine drug release by UPLC. An overview of results is presented for each of the hydrophobic repeating unit groups (Figure 3). We observe that MA- and CHA-based copolymers do not exhibit an enhanced effect on API dissolution relative to the HPA homopolymer (Figure 3A,B). However, incorporation of BA and HA into the polymer backbone enabled

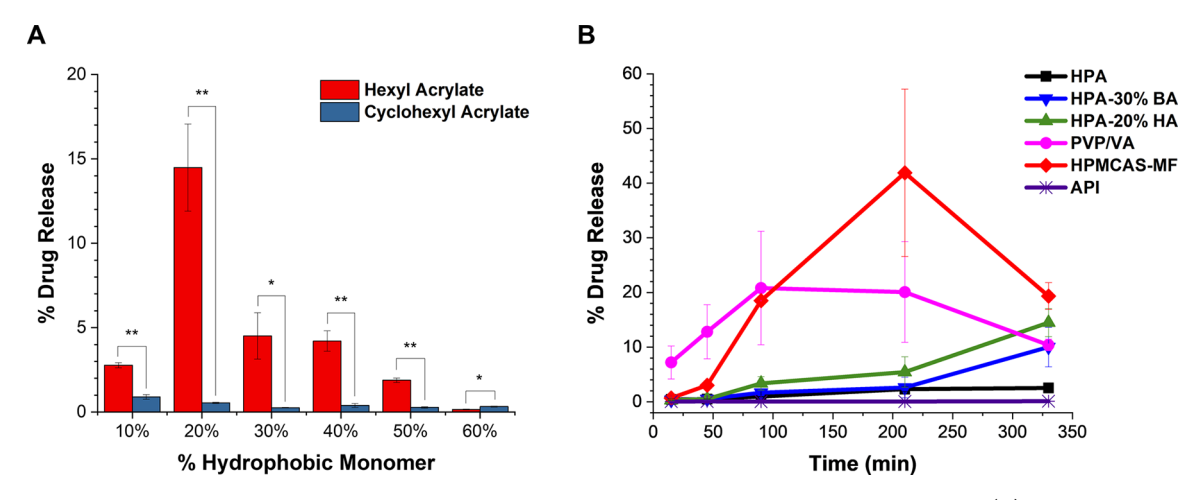


Figure 4. Comparison of API formulation ability of synthesized polymers and inclusion of conventional polymers. (A) Comparison of dissolution performance of HPA copolymers incorporated with HA and CHA monomers at t = 330 min. Drug release was quantified by UPLC and obtained by running standard injections of API. Statistical significance was determined by the student's t test where * is p < 0.05 and ** is p < 0.01. (B) HPA homopolymer and two of the top random heteropolymers synthesized (HPA-30% BA and HPA-20% HA) are displayed alongside standard polymer excipients PVP/VA and HPMCAS-MF. The concentration was quantified by UPLC by running standard injections of the API probucol. Experiments were completed in triplicate as error bars represent the standard error.

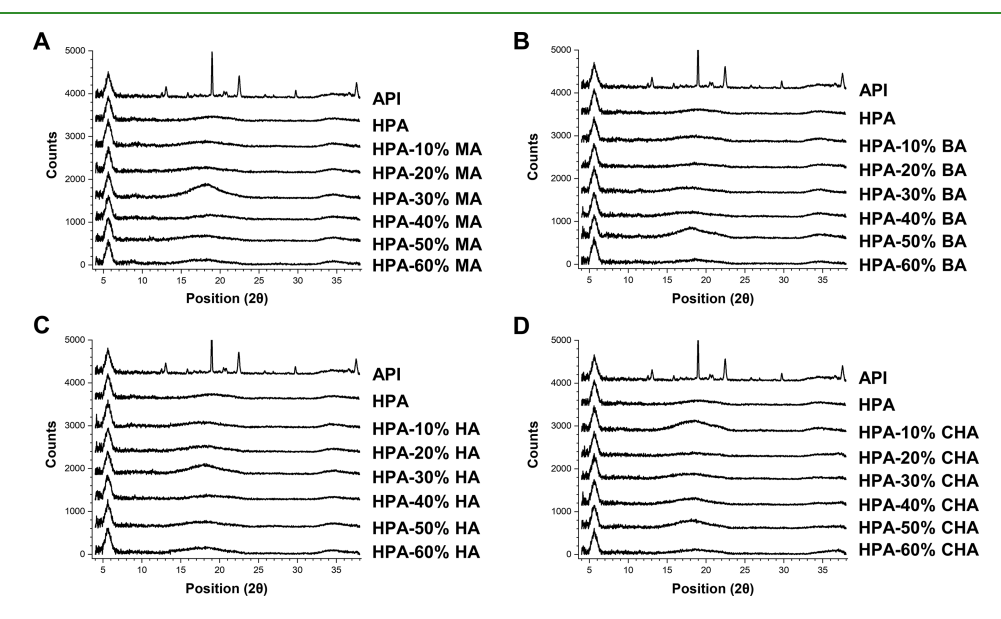


Figure 5. Transmission XRD profiles of film casted polymer/drug mixtures. XRD profiles are grouped by hydrophobic monomer incorporation: (A) MA, (B) BA, (C) HA, and (D) CHA at 20 wt % drug loading. At the time of collection, the amorphous to crystalline form conversion of polymer/drug films was not observed.

supersaturation of probucol to a greater extent than HPA homopolymer, achieving a drug release of about 15% in FaSSIF (Figure 3C,D). These results demonstrate that an optimal level of hydrophobicity in terms of alkyl side chain length and mol % incorporation of hydrophobic monomer is necessary to improve solubility of API. Further UPLC data, including standard curves of probucol and representative injections can be found in Figures S3—S5.

To further understand these trends, we compared synthesized polymers and included conventional polymers in the experimental design (Figure 4). Hydrophobicity cannot be the only driving factor as the presence of CHA monomer, which has a similar log *P* as HA and an equal number of carbon atoms on the side chain as HA (Figure 2), did not boost API dissolution significantly at the various mol % levels investigated in this study (Figure 3B). A comparison of dissolution performance of

copolymers containing equivalent percentages of HA and CHA, two monomers that have similar hydrophobicity but varied geometry, is shown (Figure 4A). When comparing the two groups of copolymers, HA copolymers lead to a statistically significant improvement in dissolution performance of probucol over CHA copolymers from 10 to 50 mol % hydrophobic monomer. At 60 mol % hydrophobic monomer, both display a minimal effect. We then compared the performance of the two highest performing random heteropolymers (HPA-30% BA and HPA-20% HA) synthesized in this study to the conventional polymers: PVP/VA and HPMCAS-MF (Figure 4B). Compared to PVP/VA and HPMCAS-MF, the synthesized polyacrylate copolymers have slower drug release kinetics and can achieve a comparable level of drug supersaturation as PVP/VA and HPMCAS-MF polymers by the 330 min time point.

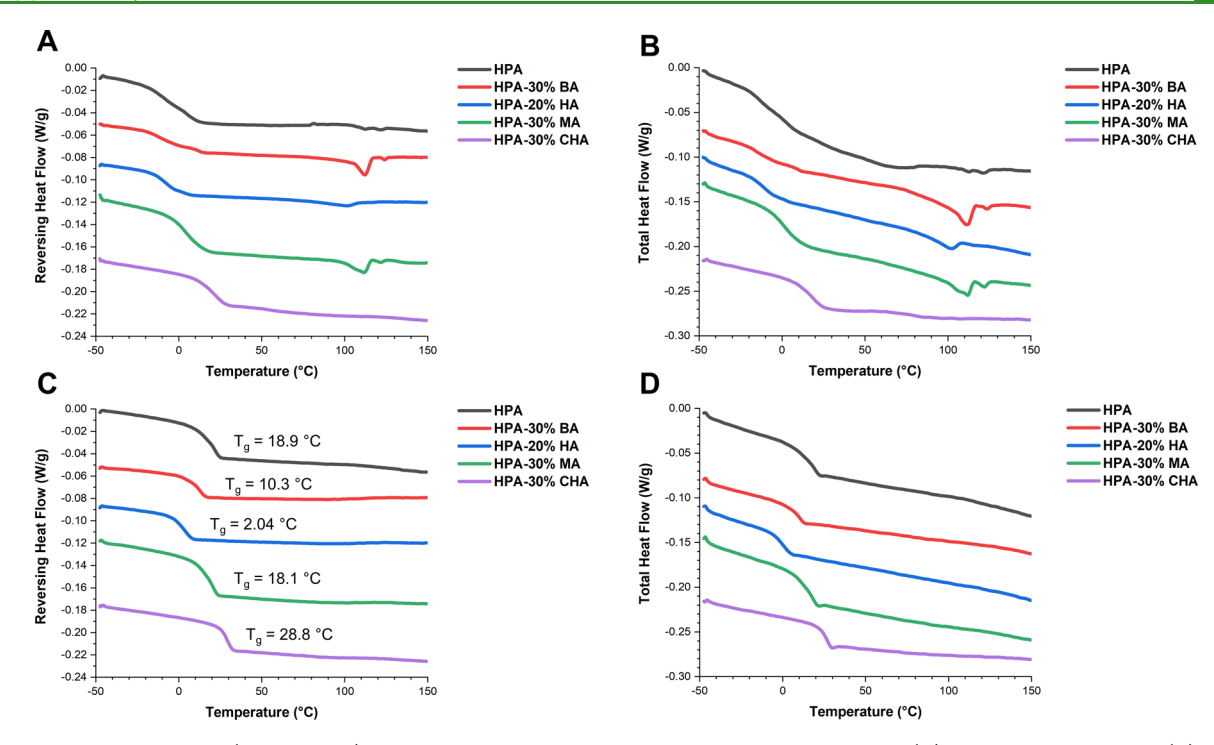


Figure 6. mDSC thermograms (exotherm up) for selected polymer/probucol films. mDSC first heat cycle (A) reversing heat flow and (B) total heat flow plots along with second heat cycle (C) reversing heat flow and (D) total heat flow plots for polymer loaded with 20 wt % API. The representative polymers displayed are HPA homopolymer, HPA-30% BA, HPA-20% HA, HPA-30% MA, and HPA-30% CHA. Respective $T_{\rm g}$ values are displayed for the second heat cycle (C). There is a varying degree of crystallinity and miscibility of polymer and drug exhibited.

Transmission XRD analysis was performed for all polymer/drug films after solvent evaporation to assess the amorphous to crystalline form conversion of probucol after the formation of film casted ASDs and prior to initiation of dissolution analysis (Figure 5). For all groups of hydrophobic monomers that were incorporated into the copolymer, the amorphous to crystalline form conversion of probucol prior to dissolution analysis was not observed via transmission XRD.

mDSC was performed for each film casted polymer/drug mixture after 48 h of ambient storage. We have highlighted the DSC reversing heat flow thermograms of some key synthesized polymer excipients (HPA homopolymer, HPA-30% BA, HPA-20% HA, HPA-30% MA, and HPA-30% CHA) along with the respective T_g values calculated from the second heat cycle (Figure 6). These film casted samples demonstrated a single $T_{\rm g}$ region and melting endotherms showing the amorphous to crystalline form conversion of probucol over 48 h of ambient storage (Figure 6A). Also, no recrystallization exotherms were observed in the total heat flow thermogram during the first heat cycle (Figure 6B). To reduce any potential solvent effects, a second heat cycle was completed with the reversing heat flow (Figure 6C) and total heat flow (Figure 6D) as shown. Cooling cycle or second heat cycle thermograms did not show recrystallization exotherms or subsequent melting endotherms, indicating the drug did not recrystallize during the cooling cycle. Moreover, a single narrow T_g was observed in all cases during the second heat cycle and in the majority of cases in the first heat cycle in DSC, indicating miscibility of probucol in these polymers (Figures S8-S10). However, further analysis would be needed to ascertain nanoscale level miscibility. Additional mDSC thermograms for polymers and polymer/probucol films are included in Figures S8–S10 along with second heat cycle T_{σ} values for polymer/probucol films in Table S2.

To further assess any amorphous to crystalline form conversion of probucol prior to dissolution characterization,

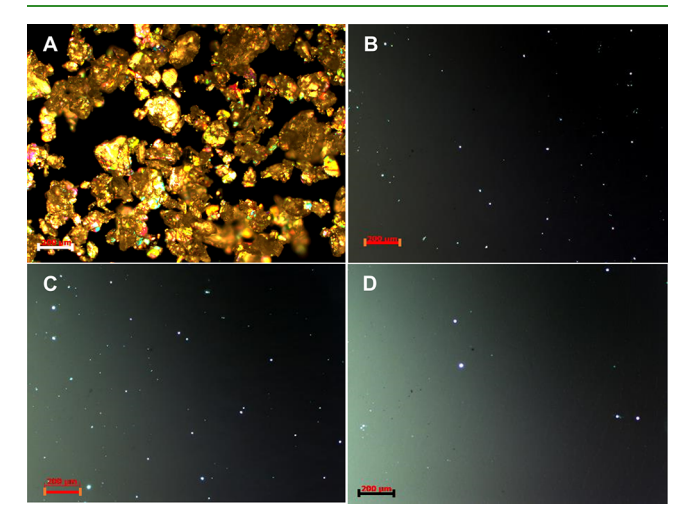


Figure 7. Polarized light microscopy contrasting crystalline API probucol to amorphous polymer/drug formulations. (A) Probucol was prepared in acetone and diluted into PBS (2 vol % acetone) and subsequently film casted onto a glass slide. Polymer/drug mixtures prepared in acetone and film casted directly include (B) HPA homopolymer, (C) HPA-30% BA, and (D) HPA-20% HA with 20 wt % probucol. The scale bar represents 200 μm.

we obtained polarized light microscopy images of polymerdrug films casted separately onto individual glass slides (Figure 7). Glass slides were used to reduce background noise. The API probucol was prepared by initially dissolving in acetone and diluting into PBS (2 vol % acetone) (Figure 7A). We also collected images of API formulated with HPA homopolymer

(Figure 7B), HPA-30% BA (Figure 7C), and HPA-20% HA (Figure 7D). All samples were given time to evaporate fully and were immediately imaged. The bright spots observed in Figures 7B–D are background associated with the slides.

On the basis of these characteristics of probucol, we designed random heteropolymers containing a hydrophilic monomer (HPA) with hydroxyl groups to enable hydrogen-bonding interactions with probucol that can mitigate precipitation of probucol from amorphous (in ASD) to crystalline form in solution. To explore the impact of hydrophobicity or amphiphilic balance of a polymer on solubility enhancement of probucol, we systematically varied the copolymer hydrophobicity through incorporation of alkyl side groups with varying length (methyl, butyl, and hexyl) and mol % to potentially interact with the API via hydrophobic interactions. 17,19 Furthermore, copolymers with 0–60 mol % of cyclohexyl side groups were synthesized to explore the role of polymer side group geometry on probucol supersaturation in ASDs. We hypothesize that the side group geometry at some hydrophobicity level (in terms of the number of carbon atoms) can impact polymer chain flexibility and steric hindrance which can play a role in polymer-drug interactions in solution and solid state. This approach can be utilized to conduct a high throughput screening of large polymer libraries to identify highperforming polymer excipients and recognize structurefunction relationships.

These selected hydrophobic monomers are structurally diverse in that MA, BA, and HA contain side group alkyl chains that are one, four, and six carbons in length, respectively, while CHA contains a cyclohexyl side group. These monomers were also selected because they have a wide range of $\log P$ as MA has a $\log P$ similar to HPA ($\log P = 0.62$), and HA exhibits the greatest hydrophobicity of the five monomers ($\log P = 3.14$). Previous work suggests that polymer solubility can become an issue at about $\log P > 1.00$, 52 so we designed random heteropolymers of HPA containing 0–60 mol % hydrophobic monomer. The weighted $\log P$ values of these synthesized random heteropolymers range from 0.64 to 2.13, encompassing the expected polymer solubility.

In these controlled polymerizations (D < 1.26), molecular weights quantified by GPC trended lower compared to theoretical molecular weights while agreeing with molecular weights determined by NMR (Table 1). If greater conversion is required, the polymerization time can likely be increased along with further characterization of reactivity ratios.⁵⁵ HPA homopolymer was observed to have a $T_{\rm g}$ of 23 °C while random heteropolymers containing MA, BA, HA, and CHA had $T_{\rm g}$ ranges of about 19 to 23, -17 to 18, -9 to 15, and 24 to 30 °Č, respectively. CHA incorporation likely resulted in the greatest T_g range because CHA has high rigidity, steric hindrance, and dimensional stability compared to the other hydrophobic monomers which have flexible alkyl side chains. 56 It is also appropriate that the length of the alkyl side chain for approximately equal molecular weight polymers is inversely proportional to $T_{\rm g}$. Incorporation of monomers with longer alkyl chains (e.g., HA) results in a higher free volume which corresponds to decreased $T_{\rm g}$. ^{57,58} A major aspect of the synthesis workflow was purification of small molecule impurities (ZnTPP) and monomers) which was completed by using desalting plates loaded with size-exclusion resin. Our group has previously validated this technique for removal of ZnTPP, demonstrating a removal efficiency of about 84% in one purification step and 96% in three purification steps. Depending on sensitivity, biological

studies may require at least three purification steps or purification by precipitation which was shown to remove all measurable ZnTPP.

Other interesting trends were observed with regard to API dissolution performance. BA- and HA-based copolymers demonstrated a gradual increase in probucol supersaturation up to an optimal mol % of hydrophobic comonomer followed by a substantial drop in dissolution performance of probucol as further mol % of hydrophobic BA and HA comonomers were incorporated (Figure 3). In these two copolymer series, the highest improvement in probucol dissolution was achieved at 30 mol % of hydrophobic comonomer in BA-based copolymers and 20 mol % of hydrophobic comonomer in HA-based copolymers (Figure 3C,D). As BA and HA incorporation increased, the detected API concentrations shift in a stepwise fashion similar to a bell curve. When comparing the estimated log P values of the HPA-30% BA and HPA-20% HA polymers that best achieved probucol supersaturation, we found that the weighted average monomer log P values are nearly identical at 1.12 and 1.14, respectively (Table 1).

In comparison to these two high-performing copolymer compositions in this study, the estimated log P values for copolymers with methyl side groups were all substantially lower than BA and HA series copolymers. Even a high mol % (60 mol %) of the shorter methyl alkyl group in the copolymer did not lead to any significant improvement in dissolution of probucol. This observation is aligned with estimated log P values that appear similar across the MA copolymer series. The role of hydrophobicity in solution performance of ASDs has been investigated earlier, but the systematic investigation in this study shows that longer alkyl side groups at a lower mol % in copolymers can be most effective in enhancing the aqueous solubility and potentially the oral bioavailability of hydrophobic drugs similar to probucol. Our results on HA and BA copolymers show the minor changes in copolymer composition can have a tremendous impact on polymer performance as a shift from an optimal mol % of 20 mol % HA and 30 mol % BA led to substantial reduction in probucol dissolution. This substantiates both shortcomings and opportunities related to customizing conventional polymers such as HPMCAS which can have a wide range of functional group substitution within the polymer grade. Random heteropolymer hydrophobicity likely plays a key role in formulating probucol due to a balance of hydrophobic and hydrogen-bonding interactions between polymer and API. 18,19

Interestingly, even though both HA and CHA monomers have the same number of carbon atoms in the side group and similar log P values, there is a dramatic difference in solution performance of copolymers based on these repeating units toward probucol dissolution enhancement (Figure 4A). This supports that, in addition to hydrophobicity, hydrophobic side chain geometry plays a crucial role in attaining supersaturation of probucol as long, flexible alkyl side chains performed best. The steric hindrance due to bulky CHA side groups as compared to linear HA side groups can increase the polymer chain rigidity (also evident by higher T_g of CHA-based copolymers) and hinder the copolymer-drug interaction or nanoaggregate formation ability in solution. Additionally, at 60 mol % hydrophobic monomer, both random heteropolymers result in minimal formulation capability, indicating that 10-50 mol % of HA may represent an optimal hydrophobicity range (0.89 < log P < 1.89). To further explore the effect of side chain geometry, other hydrophobic monomers could potentially be utilized such as phenyl acrylate.

The two highest performing synthesized polymers (HPA-30% BA and HPA-20% HA) were then compared to industry standard polymers (Figure 4B). These standard polymer excipients (HPMCAS-MF and PVP/VA) exhibited a rapid release profile associated with their known "spring and parachute effect" whereby there is rapid initial supersaturation (spring) followed by inhibition or slow API precipitation (parachute). 59-61 In contrast, the drug release kinetics associated with the two synthesized polymers revealed a slow, gradual dissolution with an ability to maintain supersaturation up to at least 330 min (parachute). Other works have utilized modified HPMCAS, different monomer side groups (e.g., carboxylic acid), and charged polymers which typically present a spring and parachute profile. 15,16,18,19 It is intriguing that a combinatorial library approach with focused exploration of multiple hydrophobic monomers has yielded slower API dissolution with steady supersaturation. Nevertheless, through this approach we have demonstrated the ability to modulate the release of hydrophobic API through systematic optimization of copolymer architecture and the dramatic role of alkyl side group geometry on dissolution characteristics of a hydrophobic drug.

In addition to the film casting screen, characterization methods to determine solid-state stability included XRD, mDSC, and polarized light microscopy. By XRD, we observed a lack of crystalline peaks for all polymer/drug films (Figure 5). For analogous polymers at comparable probucol drug loading, a similar result was found by Reineke and co-workers indicating the ability of synthetic polymers to achieve molecularly dispersed drug within the sensitivity limit of these analytical techniques. In fact, more pronounced crystallinity would be expected at about 50 wt % drug loading. 15,18,19 The mDSC profiles for some highlighted polymers (Figure 6) suggest miscibility and interaction between polymer and API due to the single glass transitions observed. As expected, T_{σ} 's of polymer/ drug films were lower relative to the respective polymers because of plasticization.⁶²⁻⁶⁵ Note that the second heat cycle was utilized to determine $T_{\rm g}$ to ensure that there would be no effect from residual solvent that may be present. A broad melting endotherm was found between about 100 and 120 °C, potentially because probucol recrystallized into different polymorphs. 19,66-68 The data also indicate that API already crystallized after two or more days because no recrystallization exotherm was observed. Limited physical stability of these film casted ASDs can be attributed to the low T_g of the synthesized polyacrylates. Even though the main objective of this study was to assess the role of polymer structural attributes on solution performance of solid dispersions, improvement in physical stability by potentially enhancing $T_{\rm g}$ will be advantageous for applications in pharmaceutical drug product development. Further investigations are underway to enhance $T_{\rm g}$ of these polymer structures by increasing polymer backbone rigidity.

Presented by Ting et al., a major concern in the field of designer polymer formulations is developing overcomplicated processes for polymer design and synthesis. As a solution, our automated synthetic approach offers end-user functionality with minimal training and batch-to-batch reproducibility. The objective of this study is to provide a framework for others through which an automated combinatorial library workflow can be implemented to uncover the importance of various polymer structural properties. In work, polymer design can be more precisely defined by incorporating conjugation techniques, 38,39 nonlinear architectures, 38 and stereochemical control. Improved statistical control over polymer composition can be

accomplished by quantifying monomer reactivity ratios and modeling compositional drift. $^{70-72}$ Recently, fascinating developments have been made in applying automated liquid handling technology to screen polymers for their ability to inhibit API precipitation. 20 Another beneficial future strategy would be to combine automated synthesis and screening because it would enable testing various API functionalities, drug loading wt %, target drug concentration, and buffer conditions. Overall, we have demonstrated the potential of an automated polymer synthesis and combinatorial library approach to rapidly assess API supersaturation. In doing so, we found a relationship between polymer hydrophobicity, side group geometry, and dissolution performance with slower release kinetics relative to standard excipients. Ultimately, we believe that the importance of various polymer structural parameters can be elucidated by supplementing high throughput combinatorial and screening techniques with quantitative modeling. Through this work, we hope to make the oral drug delivery community aware of the utility of automated combinatorial polymer synthesis.

4. CONCLUSION

In conclusion, we demonstrated that automated combinatorial polymer synthesis in combination with a rapid ASD screening approach can be applied to the oral drug delivery community in developing designer polymer excipients. Once the polymer library was fed into a rapid film casting screen, we uncovered significant relationships between polymer hydrophobicity, side chain geometry, and the ability to achieve supersaturation of the model drug probucol. We further communicated that longer, flexible alkyl hydrophobic side chains outperformed cyclohexyl side groups in API dissolution. Lastly, the two most effective synthesized polymer excipients surprisingly displayed a slower, more gradual release profile relative to industry standard polymers, signifying the ability of this system to control drug release. In the future, a successful strategy in this space would likely involve combining automated, high throughput synthesis and screening with quantitative modeling. This is an exciting time for the oral drug delivery community which now has the required tools to begin specifying structure-activity relationships for designer polymer excipients.

ASSOCIATED CONTENT

Supporting Information

The Supporting Information is available free of charge at https://pubs.acs.org/doi/10.1021/acsapm.0c01376.

Polymer structures, GPC data, UPLC data, mDSC data, and ¹H NMR data (PDF)

AUTHOR INFORMATION

Corresponding Authors

Adam J. Gormley — Department of Biomedical Engineering, Rutgers, The State University of New Jersey, Piscataway, New Jersey 08854, United States; oorcid.org/0000-0002-2884-725X; Email: Adam.Gormley@rutgers.edu

Ashish Punia — Preformulation Sciences, MRL, Merck & Co., Inc., Rahway, New Jersey 07065, United States; Email: Ashish.Punia@merck.com

Authors

Rahul Upadhya – Department of Biomedical Engineering, Rutgers, The State University of New Jersey, Piscataway, New

- Jersey 08854, United States; o orcid.org/0000-0002-6268-8029
- Mythili J. Kanagala Department of Biomedical Engineering, Rutgers, The State University of New Jersey, Piscataway, New Jersey 08854, United States
- Lina Liu Preformulation Sciences, MRL, Merck & Co., Inc., Rahway, New Jersey 07065, United States
- Matthew Lamm Preformulation Sciences, MRL, Merck & Co., Inc., Rahway, New Jersey 07065, United States; ⊚ orcid.org/0000-0002-2787-0642
- Timothy A. Rhodes Preformulation Sciences, MRL, Merck & Co., Inc., Rahway, New Jersey 07065, United States

Complete contact information is available at: https://pubs.acs.org/10.1021/acsapm.0c01376

Notes

The authors declare no competing financial interest.

ACKNOWLEDGMENTS

R.U. was supported by the National Institutes of General Medical Sciences of the National Institutes of Health under Award T32 GM008339. R.U. was also supported by the New Jersey Commission on Cancer Research (NJCCR) Pre-Doctoral Research Fellowship under the New Jersey Department of Health. Additional support was provided by NSF CBET Award 2009942.

REFERENCES

- (1) Ting, J. M.; Porter, W. W., III; Mecca, J. M.; Bates, F. S.; Reineke, T. M. Advances in Polymer Design for Enhancing Oral Drug Solubility and Delivery. *Bioconjugate Chem.* **2018**, *29*, 939–952.
- (2) Ahn, H.; Park, J. H. Liposomal Delivery Systems for Intestinal Lymphatic Drug Transport. *Biomater. Res.* **2016**, 20, 1–6.
- (3) Loftsson, T.; Brewster, M. E. Pharmaceutical Applications of Cyclodextrins: Basic Science and Product Development. *J. Pharm. Pharmacol.* **2010**, *62*, 1607–1621.
- (4) Thompson, L. A.; Ellman, J. A. Synthesis and Applications of Small Molecule Libraries. *Chem. Rev.* **1996**, *96*, 555–600.
- (5) Gordon, E. M.; Gallop, M. A.; Patel, D. V. Strategy and Tactics in Combinatorial Organic synthesis. Applications to Drug Discovery. *Acc. Chem. Res.* **1996**, *29*, 144–154.
- (6) Balkenhohl, F.; von dem Bussche-Hünnefeld, C.; Lansky, A.; Zechel, C. Combinatorial Synthesis of Small Organic Molecules. *Angew. Chem., Int. Ed. Engl.* **1996**, *35*, 2288–2337.
- (7) Schneider, G. Automating Drug Discovery. *Nat. Rev. Drug Discovery* **2018**, *17*, 97–113.
- (8) Sarkar, A.; Kellogg, G. E. Hydrophobicity Shake Flasks, Protein Folding and Drug Discovery. *Curr. Top. Med. Chem.* **2010**, *10*, 67–83.
- (9) Pan, A. C.; Borhani, D. W.; Dror, R. O.; Shaw, D. E. Molecular Determinants of Drug-Receptor Binding Kinetics. *Drug Discovery Today* **2013**, *18*, 667–673.
- (10) Jermain, S. V.; Brough, C.; Williams, R. O. Amorphous Solid Dispersions and Nanocrystal Technologies for Poorly Water-Soluble Drug Delivery An Update. *Int. J. Pharm.* **2018**, *535*, 379–392.
- (11) Ricarte, R. G.; Van Zee, N. J.; Li, Z.; Johnson, L. M.; Lodge, T. P.; Hillmyer, M. A. Recent Advances in Understanding the Micro- and Nanoscale Phenomena of Amorphous Solid Dispersions. *Mol. Pharmaceutics* **2019**, *16*, 4089–4103.
- (12) Qian, F.; Huang, J.; Hussain, M. A. Drug-Polymer Solubility and Miscibility: Stability Consideration and Practical Challenges in Amorphous Solid Dispersion Development. *J. Pharm. Sci.* **2010**, *99*, 2941–2947.
- (13) Singh, A.; Van den Mooter, G. Spray Drying Formulation of Amorphous Solid Dispersions. *Adv. Drug Delivery Rev.* **2016**, *100*, 27–50.

- (14) Agrawal, A. M.; Dudhedia, M. S.; Zimny, E. Hot Melt Extrusion: Development of an Amorphous Solid Dispersion for an Insoluble Drug from Mini-Scale to Clinical Scale. *AAPS PharmSciTech* **2016**, *17*, 133–147
- (15) Dalsin, M. C.; Tale, S.; Reineke, T. M. Solution-State Polymer Assemblies Influence BCS Class II Drug Dissolution and Supersaturation Maintenance. *Biomacromolecules* **2014**, *15*, 500–511.
- (16) Ricarte, R. G.; Li, Z.; Johnson, L. M.; Ting, J. M.; Reineke, T. M.; Bates, F. S.; Hillmyer, M. A.; Lodge, T. P. Direct Observation of Nanostructures during Aqueous Dissolution of Polymer/Drug Particles. *Macromolecules* **2017**, *50*, 3143–3152.
- (17) Tale, S.; Purchel, A. A.; Dalsin, M. C.; Reineke, T. M. Diblock Terpolymers Are Tunable and pH Responsive Vehicles To Increase Hydrophobic Drug Solubility for Oral Administration. *Mol. Pharmaceutics* **2017**, *14*, 4121–4127.
- (18) Ting, J. M.; Navale, T. S.; Bates, F. S.; Reineke, T. M. Design of Tunable Multicomponent Polymers as Modular Vehicles To Solubilize Highly Lipophilic Drugs. *Macromolecules* **2014**, 47, 6554–6565.
- (19) Ting, J. M.; Navale, T. S.; Jones, S. D.; Bates, F. S.; Reineke, T. M. Deconstructing HPMCAS: Excipient Design to Tailor Polymer-Drug Interactions for Oral Drug Delivery. ACS Biomater. Sci. Eng. 2015, 1, 978–990.
- (20) Ting, J. M.; Tale, S.; Purchel, A. A.; Jones, S. D.; Widanapathirana, L.; Tolstyka, Z. P.; Guo, L.; Guillaudeu, S. J.; Bates, F. S.; Reineke, T. M. High-Throughput Excipient Discovery Enables Oral Delivery of Poorly Soluble Pharmaceuticals. *ACS Cent. Sci.* **2016**, *2*, 748–755.
- (21) Pouton, C. W. Lipid Formulations for Oral Administration of Drugs: Non-Emulsifying, Self-Emulsifying and 'Self-Microemulsifying' Drug Delivery Systems. *Eur. J. Pharm. Sci.* **2000**, *11*, S93—S98.
- (22) Gursoy, R. N.; Benita, S. Self-Emulsifying Drug Delivery Systems (SEDDS) for Improved Oral Delivery of Lipophilic Drugs. *Biomed. Pharmacother.* **2004**, *58*, 173–182.
- (23) Wischke, C.; Schwendeman, S. P. Principles of Encapsulating Hydrophobic Drugs in PLA/PLGA Microparticles. *Int. J. Pharm.* **2008**, 364, 298–327.
- (24) Larrañeta, E.; Barturen, L.; Ervine, M.; Donnelly, R. F. Hydrogels Based on Poly(Methyl Vinyl Ether-co-Maleic Acid) and Tween 85 for Sustained Delivery of Hydrophobic Drugs. *Int. J. Pharm.* **2018**, 538, 147–158.
- (25) Motiei, M.; Kashanian, S. Novel Amphiphilic Chitosan Nanocarriers for Sustained Oral Delivery of Hydrophobic Drugs. *Eur. J. Pharm. Sci.* **2017**, *99*, 285–291.
- (26) López-Cebral, R.; Peng, G. J.; Reys, L. L.; Silva, S. S.; Oliveira, J. M.; Chen, J.; Silva, T. H.; Reis, R. L. Dual Delivery of Hydrophilic and Hydrophobic Drugs from Chitosan/Diatomaceous Earth Composite Membranes. *J. Mater. Sci.: Mater. Electron.* **2018**, *29*, 1–12.
- (27) Li, Y. Y.; Qiu, X. Q.; Qian, Y.; Xiong, W. L.; Yang, D. J. pH-Responsive Lignin-Based Complex Micelles: Preparation, Characterization and Application in Oral Drug Delivery. *Chem. Eng. J.* **2017**, 327, 1176–1183.
- (28) Delmar, K.; Bianco-Peled, H. Composite Chitosan Hydrogels for Extended Release of Hydrophobic Drugs. *Carbohydr. Polym.* **2016**, *136*, 570–580.
- (29) Sarabu, S.; Kallakunta, V. R.; Bandari, S.; Batra, A.; Bi, V.; Durig, T.; Zhang, F.; Repka, M. A. Hypromellose Acetate Succinate Based Amorphous Solid Dispersions via Hot Melt Extrusion: Effect of Drug Physicochemical Properties. *Carbohydr. Polym.* **2020**, 233, 115828.
- (30) Huang, W. J.; Mandal, T.; Larson, R. G. Computational Modeling of Hydroxypropyl-Methylcellulose Acetate Succinate (HPMCAS) and Phenytoin Interactions: A Systematic Coarse-Graining Approach. *Mol. Pharmaceutics* **2017**, *14*, 733–745.
- (31) Balogh, A.; Farkas, B.; Pálvolgyi, A.; Domokos, A.; Démuth, B.; Marosi, G.; Nagy, Z. K. Novel Alternating Current Electrospinning of Hydroxypropylmethylcellulose Acetate Succinate (HPMCAS) Nanofibers for Dissolution Enhancement: The Importance of Solution Conductivity. *J. Pharm. Sci.* **2017**, *106*, 1634–1643.
- (32) Huang, W. J.; Mandal, T.; Larson, R. G. Multiscale Computational Modeling of the Nanostructure of Solid Dispersions of

- Hydroxypropyl Methylcellulose Acetate Succinate (HPMCAS) and Phenytoin. *Mol. Pharmaceutics* **2017**, *14*, 3422–3435.
- (33) Wang, S.; Liu, C. Y.; Chen, Y. J.; Zhu, A.; Qian, F. Aggregation of Hydroxypropyl Methylcellulose Acetate Succinate under Its Dissolving pH and the Impact on Drug Supersaturation. *Mol. Pharmaceutics* **2018**, 15, 4643–4653.
- (34) Webster, O. W. Living Polymerization Methods. *Science* **1991**, 251, 887–893.
- (35) Cole, J. P.; Hanlon, A. M.; Rodriguez, K. J.; Berda, E. B. Protein-Like Structure and Activity in Synthetic Polymers. *J. Polym. Sci., Part A: Polym. Chem.* **2017**, *55*, 191–206.
- (36) Vandermeulen, G. W. M.; Klok, H. A. Peptide/Protein Hybrid Materials: Enhanced Control of Structure and Improved Performance Through Conjugation of Biological and Synthetic Polymers. *Macromol. Biosci.* **2004**, *4*, 383–398.
- (37) Varma, A. J.; Kennedy, J. F.; Galgali, P. Synthetic Polymers Functionalized by Carbohydrates: A Review. *Carbohydr. Polym.* **2004**, *56*, 429–445.
- (38) Gormley, A. J.; Yeow, J.; Ng, G.; Conway, O.; Boyer, C.; Chapman, R. An Oxygen-Tolerant PET-RAFT Polymerization for Screening Structure-Activity Relationships. *Angew. Chem., Int. Ed.* **2018**, *57*, 1557–1562.
- (39) Li, Z. H.; Kosuri, S.; Foster, H.; Cohen, J.; Jumeaux, C.; Stevens, M. M.; Chapman, R.; Gormley, A. J. A Dual Wavelength Polymerization and Bioconjugation Strategy for High Throughput Synthesis of Multivalent Ligands. *J. Am. Chem. Soc.* **2019**, *141*, 19823–19830.
- (40) Yeow, J.; Chapman, R.; Gormley, A. J.; Boyer, C. Up in the Air: Oxygen Tolerance in Controlled/Living Radical Polymerisation. *Chem. Soc. Rev.* **2018**, *47*, 4357–4387.
- (41) Oliver, S.; Zhao, L.; Gormley, A. J.; Chapman, R.; Boyer, C. Living in the Fast Lane High Throughput Controlled/Living Radical Polymerization. *Macromolecules* **2019**, *52*, 3–23.
- (42) Johnson, L. M.; Hillmyer, M. A. Critical Excipient Properties for the Dissolution Enhancement of Phenytoin. ACS Omega 2019, 4, 19116–19127.
- (43) Johnson, L. M.; Li, Z.; LaBelle, A. J.; Bates, F. S.; Lodge, T. P.; Hillmyer, M. A. Impact of Polymer Excipient Molar Mass and End Groups on Hydrophobic Drug Solubility Enhancement. *Macromolecules* **2017**, *50*, 1102–1112.
- (44) Frank, D. S.; Zhu, Q. Y.; Matzger, A. J. Inhibiting or Accelerating Crystallization of Pharmaceuticals by Manipulating Polymer Solubility. *Mol. Pharmaceutics* **2019**, *16*, 3720–3725.
- (45) Enciso, A. E.; Fu, L. Y.; Russell, A. J.; Matyjaszewski, K. A Breathing Atom-Transfer Radical Polymerization: Fully Oxygen-Tolerant Polymerization Inspired by Aerobic Respiration of Cells. *Angew. Chem., Int. Ed.* **2018**, *57*, 933–936.
- (46) Chapman, R.; Gormley, A. J.; Herpoldt, K. L.; Stevens, M. M. Highly Controlled Open Vessel RAFT polymerizations by Enzyme Degassing. *Macromolecules* **2014**, *47*, 8541–8547.
- (47) Chapman, R.; Gormley, A. J.; Stenzel, M. H.; Stevens, M. M. Combinatorial Low-Volume Synthesis of Well-Defined Polymers by Enzyme Degassing. *Angew. Chem., Int. Ed.* **2016**, *55*, 4500–4503.
- (48) Xu, J. T.; Jung, K.; Atme, A.; Shanmugam, S.; Boyer, C. A Robust and Versatile Photoinduced Living Polymerization of Conjugated and Unconjugated Monomers and Its Oxygen Tolerance. *J. Am. Chem. Soc.* **2014**, *136*, 5508–5519.
- (49) Yeow, J.; Chapman, R.; Xu, J. T.; Boyer, C. Oxygen Tolerant Photopolymerization for Ultralow Volumes. *Polym. Chem.* **2017**, *8*, 5012–5022.
- (50) Ng, G.; Yeow, J.; Xu, J. T.; Boyer, C. Application of Oxygen Tolerant PET-RAFT to Polymerization-Induced Self-Assembly. *Polym. Chem.* **2017**, *8*, 2841–2851.
- (51) Yeow, J.; Shanmugam, S.; Corrigan, N.; Kuchel, R. P.; Xu, J. T.; Boyer, C. A Polymerization-Induced Self-Assembly Approach to Nanoparticles Loaded with Singlet Oxygen Generators. *Macromolecules* **2016**, *49*, 7277–7285.
- (52) Upadhya, R.; Murthy, N. S.; Hoop, C. L.; Kosuri, S.; Nanda, V.; Kohn, J.; Baum, J.; Gormley, A. J. PET-RAFT and SAXS: High

- Throughput Tools To Study Compactness and Flexibility of Single-Chain Polymer Nanoparticles. *Macromolecules* **2019**, *52*, 8295–8304.
- (53) Tamasi, M.; Kosuri, S.; DiStefano, J.; Chapman, R.; Gormley, A. J. Automation of Controlled/Living Radical Polymerization. *Adv. Intell. Syst.* **2020**, *2*, 1–8.
- (54) Upadhya, R.; Kanagala, M. J.; Gormley, A. J. Purifying Low-Volume Combinatorial Polymer Libraries with Gel Filtration Columns. *Macromol. Rapid Commun.* **2019**, *40*, 1900528.
- (55) Biryan, F.; Demirelli, K. Copolymerization of Benzyl Methacrylate and a Methacrylate Bearing Benzophenoxy and Hydroxyl Side Groups: Monomer Reactivity Ratios, Thermal Studies and Dielectric Measurements. *Fibers Polym.* **2017**, *18*, 1629–1637.
- (56) Eggenhuisen, T. M.; Becer, C. R.; Fijten, M. W. M.; Eckardt, R.; Hoogenboom, R.; Schubert, U. S. Libraries of Statistical Hydroxypropyl Acrylate Containing Copolymers with LCST Properties Prepared by NMP. *Macromolecules* **2008**, *41*, 5132–5140.
- (57) White, R. P.; Lipson, J. E. G. Polymer Free Volume and Its Connection to the Glass Transition. *Macromolecules* **2016**, *49*, 3987–4007
- (58) Zhang, H.; Sun, D. D.; Peng, Y.; Huang, J. H.; Luo, M. B. Diffusivity and Glass Transition of Polymer Chains in Polymer Nanocomposites. *Phys. Chem. Chem. Phys.* **2019**, *21*, 23209–23216.
- (59) Augustijns, P.; Brewster, M. E. Supersaturating Drug Delivery Systems: Fast is not Necessarily Good Enough. *J. Pharm. Sci.* **2012**, *101*, 7—0
- (60) Bavishi, D. D.; Borkhataria, C. H. Spring and Parachute: How Cocrystals Enhance Solubility. *Prog. Cryst. Growth Charact. Mater.* **2016**, *62*, 1–8.
- (61) Liu, C. Y.; Chen, Z.; Chen, Y. J.; Lu, J.; Li, Y.; Wang, S. J.; Wu, G. L.; Qian, F. Improving Oral Bioavailability of Sorafenib by Optimizing the "Spring" and "Parachute" Based on Molecular Interaction Mechanisms. *Mol. Pharmaceutics* **2016**, *13*, 599–608.
- (62) Gutiérrez-Rocca, J. C.; McGinity, J. W. Influence of Water-Soluble and Insoluble Plasticizers on the Physical and Mechanical-Properties of Acrylic Resin Copolymers. *Int. J. Pharm.* **1994**, *103*, 293–301.
- (63) Lim, H. P.; Hoag, S. W. Plasticizer Effects on Physical-Mechanical Properties of Solvent Cast Soluplus (R) Films. *AAPS PharmSciTech* **2013**, *14*, 903–910.
- (64) Penkova, A. V.; Polotskaya, G. A.; Toikka, A. M.; Kocherbitov, V. V. Effect of Residual Solvent on Physicochemical Properties of Poly(Phenylene Isophtalamide) Membrane. *Drying Technol.* **2011**, 29, 633–641.
- (65) Ping, Z. H.; Nguyen, Q. T.; Chen, S. M.; Zhou, J. Q.; Ding, Y. D. States of Water in Different Hydrophilic Polymers DSC and FTIR Studies. *Polymer* **2001**, *42*, 8461–8467.
- (66) Thybo, P.; Pedersen, B. L.; Hovgaard, L.; Holm, R.; Mullertz, A. Characterization and Physical Stability of Spray Dried Solid Dispersions of Probucol and PVP-K30. *Pharm. Dev. Technol.* **2008**, 13, 375–386.
- (67) Rexrode, N. R.; Orien, J.; King, M. D. Effects of Solvent Stabilization on Pharmaceutical Crystallization: Investigating Conformational Polymorphism of Probucol Using Combined Solid-State Density Functional Theory, Molecular Dynamics, and Terahertz Spectroscopy. J. Phys. Chem. A 2019, 123, 6937–6947.
- (68) Kawakami, K.; Ohba, C. Crystallization of Probucol from Solution and the Glassy State. *Int. J. Pharm.* **2017**, 517, 322–328.
- (69) Shanmugam, S.; Boyer, C. Stereo-, Temporal and Chemical Control through Photoactivation of Living Radical Polymerization: Synthesis of Block and Gradient Copolymers. *J. Am. Chem. Soc.* **2015**, 137, 9988–9999.
- (70) Smith, A. A. A.; Hall, A.; Wu, V.; Xu, T. Practical Prediction of Heteropolymer Composition and Drift. *ACS Macro Lett.* **2019**, *8*, 36–40.
- (71) Ting, J. M.; Navale, T. S.; Bates, F. S.; Reineke, T. M. Precise Compositional Control and Systematic Preparation of Multimonomeric Statistical Copolymers. *ACS Macro Lett.* **2013**, *2*, 770–774.
- (72) Jiang, T.; Hall, A.; Eres, M.; Hemmatian, Z.; Qiao, B. F.; Zhou, Y.; Ruan, Z. Y.; Couse, A. D.; Heller, W. T.; Huang, H.; de la Cruz, M. O.;

Rolandi, M.; Xu, T. Single-Chain Heteropolymers Transport Protons Selectively and Rapidly. *Nature* **2020**, *577*, 216–220.